

FRACTAL DIMENSIONS OF FRACTURE SURFACES OF ROCK FRAGMENTS

Akio FUJIMURA, Yasuhiko TAKAGI, Muneyoshi FURUMOTO
and Hitoshi MIZUTANI

*Department of Earth Sciences, Nagoya University,
Furo-cho, Chikusa-ku, Nagoya 464*

Abstract: Several rock-fracture experiments are carried out under the conditions of dynamic impact and static uniaxial loading. Irregularity of the fracture surfaces of basalt and dunite fragments is quantitatively described by “fractal dimension”. The fractured surfaces produced by dynamic impacts have a small fractal dimension indicating the relatively smooth surfaces. On the other hand, the fracture surfaces produced by static uniaxial loading have a large fractal dimension. In the case of the dynamic impact, basalt and dunite possess similar fractal dimensions, while in the case of static loading, they have different distributions of fractal dimension. Thus the fractal dimension of a fragment may provide a useful information on the fracture processes.

1. Introduction

The textural features of meteoritic materials are expected to carry the significant information on the physical environment which the materials have experienced in the early stage of planetary evolution. Among the textural features, the geometrical irregularity of inclusions in meteorites such as broken chondrules and lithic fragments reflects the conditions of the fracturing and subsequent mechanical abrasion processes during collision and cratering in space and/or on the parent bodies. The study of the irregularity may help to understand the mechanical conditions of the accretion of planetary bodies. It is, however, often difficult to represent the irregularity quantitatively (FUJII *et al.*, 1982). We have found that the values of the “fractal dimension” represent the irregularity associated with the degree of fracture on rocks (FURUMOTO *et al.*, 1984). In this study, we investigate the fractal geometry (MANDELBROT, 1982) of the surfaces of experimentally produced rock fragments in detail.

2. Fractal Dimension

Geometrical roughness or irregularity of a fractured rock surface is described quantitatively with the concept of “fractal”. In the following, we briefly represent the methods of obtaining the “fractal dimension” of the rock surface, because the principle of “fractal geometry” and “fractal dimension” has been described in very detail elsewhere (MANDELBROT, 1982).

The fractal geometry of a surface is characterized by a number D , called fractal



Fig. 1. Photograph of a polished surface of a dunite fractured by an impact experiment (Run No. 840505). The "islands" of the bare dunite (black spots) are shown on the plane of epoxy resin. The "coastline" is clear on the background of the thinly coated silver.

dimension. The fractal dimension is a mathematical extension of the ordinary Euclidean dimension. It ranges from 2 to 3. D equals 2, when the surface is smooth. As the surface becomes more irregular, it increases from 2 to 3. Similarly, the fractal dimension D' of a curve is given by a number of $1 \leq D' \leq 2$.

The fractal dimension D of a surface can be estimated by the "slit island analysis" (MANDELBROT *et al.*, 1984). When the rough surface with the fractal dimension D is sectioned by a plane parallel to the average trend of the surface, "islands" which are surrounded by the intersecting curves appear (see Fig. 1). These "coastlines" are of fractal dimension $D' = D - 1$. The theory of fractals (MANDELBROT, 1982) suggests the relation as follows:

$$D' = 1 - \log L / \log r, \quad (1)$$

where L is the perimeter or the length of the coastline of the island, and r is the opening of the dividers used to measure the perimeter. It is to be noted that the perimeter L is not a constant, but a function of r . The perimeter L of an island is measured by the dividers with different opening, and D' is obtained for the island.

There is another method of obtaining D' by using an area-perimeter relationship:

$$A^{1/2} \propto L^{1/D'}, \quad (2)$$

where A is the area of the island. In this method, L and A are measured by a pair of dividers with a particular opening for a large number of islands with different sizes, and D' is obtained by using eq. (2). The obtained D' or $D (= D' + 1)$ describes the fractal-character of a fractured surface on which the analyzed islands exist. In the following, we use D' for describing the irregularity of a surface.

Thus two independent methods using eq. (1) or eq. (2) are available for determination of the fractal dimension D' .

3. Experimental and Analytical Procedure

We use three kinds of materials: 1) basalt (Chausu-yama, Aichi prefecture; TAKAGI *et al.*, 1984), 2) dunite (Horoman, Hokkaido), and 3) soda-glass. They are destroyed by either high speed impact or uniaxial loading. The results of the analysis on basalt and dunite can be applied directly to natural processes, because these rock types are common in extraterrestrial materials. Soda-glass, on the other hand, is employed to compare the results of our fractal measurement and the results by other workers. The glass samples were provided by N. FUJII, who used the same glass samples to study the fractal dimension with a Kr gas absorption method (NAKAMURA *et al.*, 1985).

Table 1. Conditions of impact experiments.

Run No.	Target		Projectile		Impact velocity (m/s)	NDIS*	m_L/M_t
	Material	Mass (g)	Material	Mass (g)			
820117	Basalt	126.58	Aluminum	4.96	820	0.544	0.0874
820219	Basalt	1056.8	Aluminum	5.02	820	0.066	0.361
820519	Basalt	32.81	Aluminum	10.05	641	3.362	0.0134
820521	Basalt	1048.8	Aluminum	9.98	600	0.094	0.217
820523	Basalt	159.29	Aluminum	10.00	289	0.289	0.111
820528	Basalt	109.04	Aluminum	10.21	136	0.199	0.601
840505	Dunite	83.28	Aluminum	7.14	305	1.463	0.0393
850510	Glass	20.58	Polycarbonate	3.08	990	40.1	0.00101
850528	Glass	22.63	Polycarbonate	2.99	482	21.7	0.163

* NDIS stands for non-dimensional impact stress which is a measure of impact intensity.

High-speed impact experiments are made by using the single-stage powder gun (MIZUTANI *et al.*, 1981). Cylindrical aluminum or polycarbonate projectiles are impacted to cubes of rocks or spherical glass with velocities of 140–900 m/s. All experimental conditions are listed in Table 1. Also listed are the ratio of the mass of the largest fragment m_L and the mass of the target M_t and the non-dimensional impact stress (NDIS) defined by TAKAGI *et al.* (1984) and MIZUTANI *et al.* (in preparation, 1985). For the detail of the impact experiments and the NDIS the reader is referred to TAKAGI *et al.* (1984).

The collected fragments of basalt and dunite are 0.1–24 g in weight. The fragments of glass from two different experiments have weight in the range of 0.005–0.01 g (Run No. 850510) and 0.16–0.77 g (Run No. 850528), respectively. Since most fragments from the Run No. 850510 are too small to be analyzed by the island analysis, we used only the largest fragments. One half of these fragments are transparent and the other half are non-transparent (milky-white) due to internal cracks. The fragments from the Runs No. 850528 and No. 850423-2 are transparent.

Uniaxial deformation experiments are performed under the room conditions by using a uniaxial loading press (MASUDA, 1984). Every specimen is compressed uniaxially under the constant strain rates from 2×10^{-6} to $1 \times 10^{-4} \text{ s}^{-1}$. Experimental conditions are listed in Table 2. Some cloth is wound round the specimen to prevent fragments from refragmentation and dispersion. Fragments analyzed are 0.066–47 g in weight.

Table 2. Conditions of uniaxial loading experiments.

Run No.	Material	Shape	Sample		Strain rate (10^{-6} s^{-1})	Maximum load (KN)
			Dimension d (mm)	l		
830107-6	Basalt	Cylindrical	14.98	37.42	2	80
830107-8	Basalt	Cylindrical	15.00	37.50	20	87
830107-9	Basalt	Cylindrical	15.00	37.50	20	88
840702	Dunite	Rectangular	10.4^2	$\times 23.7$	100	18
850423-2	Glass	Spherical	25.3		100	13
850423-3	Dunite	Cylindrical	25.08	59.26	10	88



Fig. 2. Microphotograph of a polished surface of a basalt fractured by an impact experiment (Run No. 820521). The scale bar indicates 1 mm.

After the mass determination, each fragment was thinly coated with silver by the vacuum evaporation technique in order to ensure edge retention. The fragments were then moulded in epoxy resin, and polished down until the islands of the bare basalt, dunite or glass (surrounded by silver) appeared. Two examples of the islands are shown in Figs. 2 and 3.

The islands are photographed at magnifications of 40–120 through an optical reflection microscope. The coastlines of the islands were digitized by an X – Y reader within the interval of 1.0 mm on the photograph. Some fragments of dunite were photographed at a magnification of about 800 through a SEM in order to investigate the spatial distribution of cracks in these fragments. Both the coastlines and the rivers (internal cracks) are digitized by the same manner.

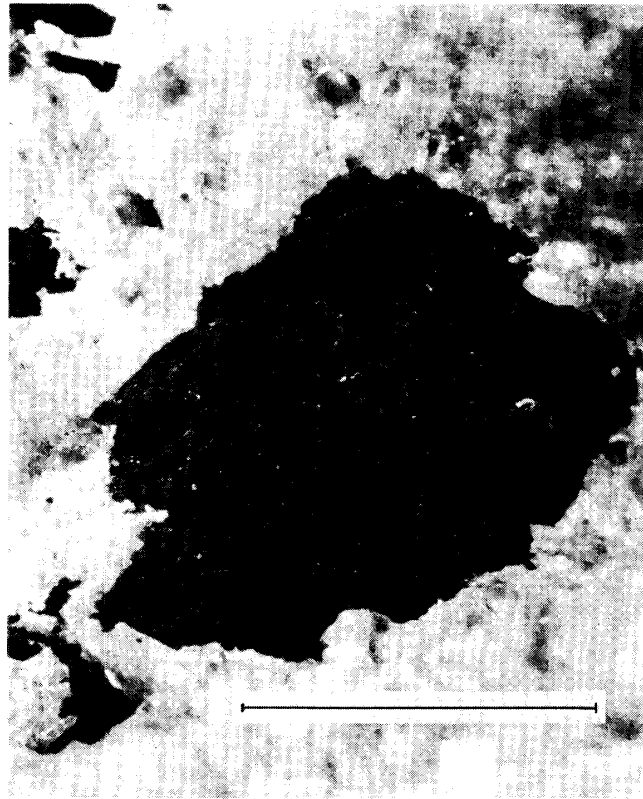


Fig. 3. Microphotograph of a polished surface of a dunite fractured by a uniaxial loading experiment (Run No. 840702). The scale bar indicates 1 mm. D' is 1.10.

The perimeter of each island is computed for a particular length of opening of the dividers. The area of the island is calculated by summing up the triangular area defined by the center of the island and both end-points of the dividers. The present procedure is basically the same as those presented in the previous literature (MANDELBROT, 1982; MANDELBROT *et al.*, 1984). We repeat the above calculation by varying the length of opening (1, 2, 4, 8 and 16 units) of the dividers. The unit size of the length of the dividers is 2.35×10^{-2} mm in real scale. We use the data of the perimeter and the area determined by the dividers with one unit length of opening for the analysis based on eq. (2), and for the analysis by eq. (1) the perimeters measured by three dividers with different openings (1, 2 and 4 units).

4. Results and Discussion

4.1. Basalt and dunite

Figure 4 shows the area-perimeter relations (eq. (2)) for the data of the impact fracture experiments with basalt (Fig. 4a) and dunite (Fig. 4b). In these figures, a linear relationship among the data covering a wide range of sizes is obvious. Very similar linear relations were obtained also for the surfaces of basalt and dunite fractured by static loading. The linear relationship demonstrates that the fractured surfaces of both basalt and dunite have the character of fractal (MANDELBROT *et al.*, 1984).

The solid lines shown in Fig. 4 represent the relationship for the fractal dimension

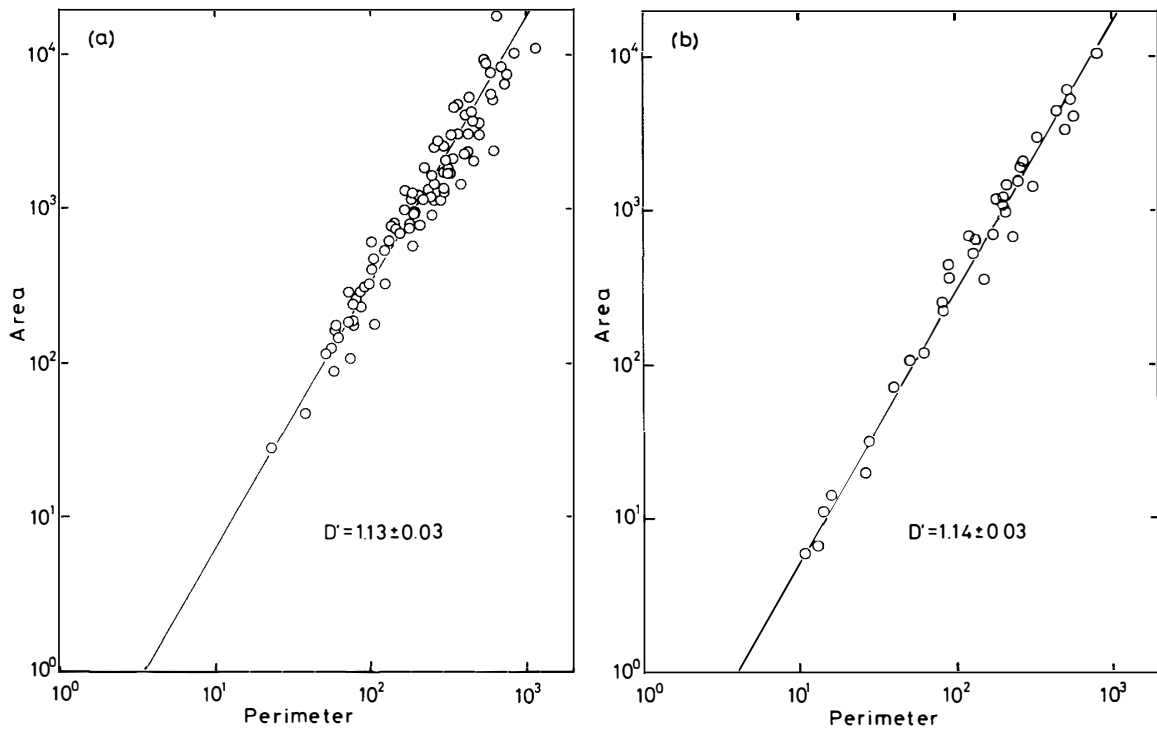


Fig. 4. Area-perimeter relationship for islands on the surfaces of an impact-fractured basalt (a) and a dunite (b). One unit of the perimeter and that of the area are 2.35×10^{-2} mm and 5.52×10^{-4} mm² in real scale, respectively.

$D' = 1.13$ and 1.14 . The similar values of the fractal dimension D' indicate that the surface irregularity of impact-fractured basalt resembles that of impact-fractured dunite. It is a striking fact that these two materials have the similar value of D' , though they have different microstructures and different mechanical properties.

In order to investigate the surface geometry in detail, we determined the fractal dimension D' of each island by using eq. (1) (Fig. 5). The total numbers of the analyzed islands are 74 (basalt) and 35 (dunite) for the samples fractured by dynamic impact, and 36 (basalt) and 24 (dunite) for the samples fractured by static uniaxial loading. The histograms of the fractal dimensions are shown in Fig. 6. The most frequently observed values are 1.08 and 1.09 for the islands on the impact-fractured surfaces of basalt and dunite, respectively (Figs. 6a and 6b). This again indicates

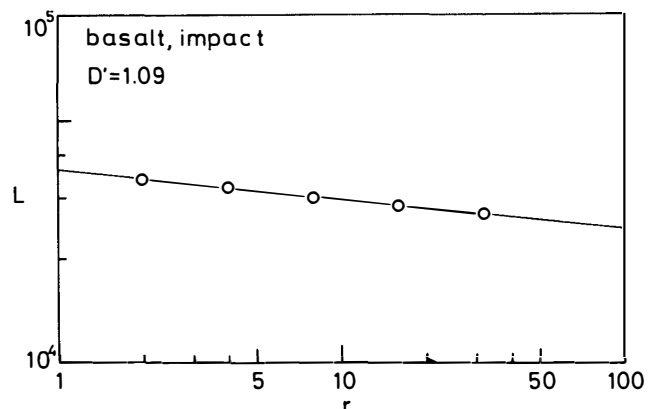


Fig. 5. The linear relation between $\log(L$; perimeter) and $\log(r$; length of opening of the dividers) on the island shown in Fig. 2.

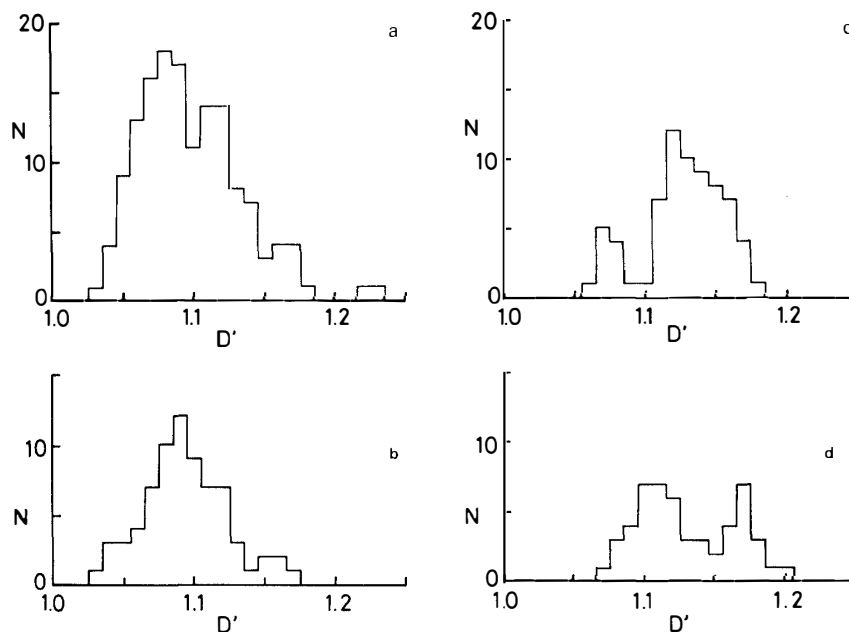


Fig. 6. Histogram of fractal dimensions D' . Left; the data for fragments of basalt (a) and dunite (b) produced by impact experiments. Right; the data for fragments of basalt (c) and dunite (d) produced by uniaxial static loading experiments.

that the surfaces of impact-fractured basalt and dunite have similar irregularity, though the values of the fractal dimension D' 's are smaller than those measured by the perimeter-area relation (eq. (2)).

In the case of the fragments produced by static loading, the most frequently observed values are 1.12 for basalt and 1.11 for dunite (Figs. 6c and 6d). In the case of dunite, however, the distribution of fractal dimensions is bimodal (Fig. 6d). Therefore, the fractal dimensions of basalt and dunite are not the same. The different physical properties of basalt and dunite may lead to the difference.

The fractal dimension of the surface produced by impact is certainly lower than that by static loading. MANDELBROT *et al.* (1984) found similar results on surfaces of "Maraging steel" fractured by "Charpy" impact and tension experiments. This relation between fracture-mode and fractal dimension might be applied to nature: we can infer the fracture-mode by investigating the fractal geometry of a rock fragment.

We investigated the spatial distribution of cracks in some islands by using the large magnification SEM image (Fig. 7a). Internal cracks in a rock fragment potentially may grow into the fracture surfaces. We suppose an extreme state in which the areas surrounded by the cracks are separated and the cracks become fracture surfaces. The fractal dimensions of some areas surrounded by cracks are calculated by using island analysis. Figure 8 shows the area-perimeter relation which indicates that the parts surrounded by cracks have the fractal geometry. Figure 9 shows the histogram of D' . The total number of the analyzed parts is 14 which are indicated as the shaded areas in Fig. 7b. The most frequently observed value of the fractal dimension D' is 1.05, which is approximately equal to $D'=1.04$ obtained from the coastline of the whole island. The above fact is interpreted as follows: when a rock fragment separates into many smaller parts by chance, they possess the similar fractal dimensions. This

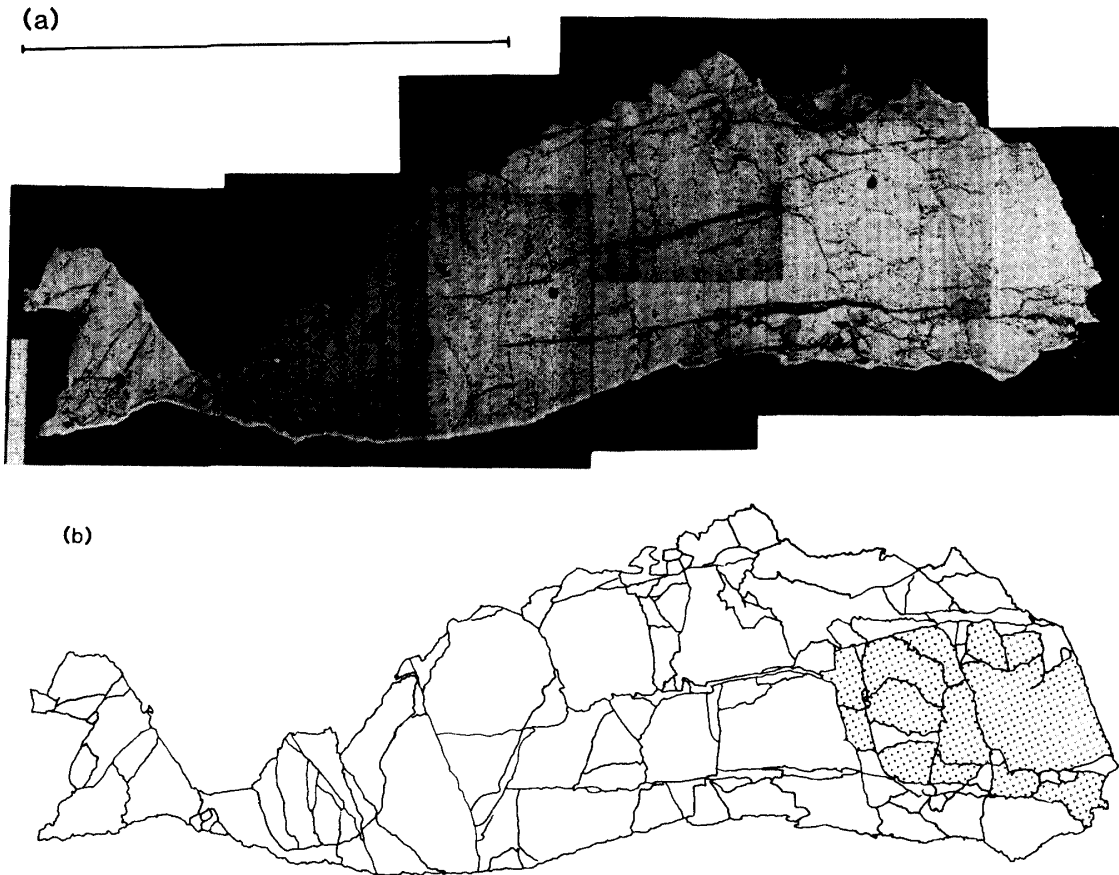


Fig. 7. (a) Microphotograph of a polished surface of a fractured dunite (Run No. 840505). The scale bar indicates 1 mm. (b) The shaded areas have been analyzed.

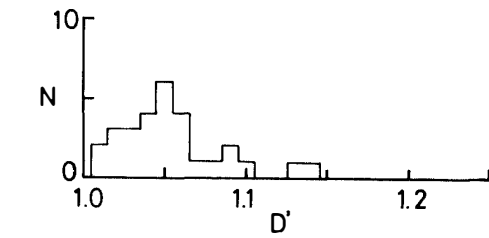
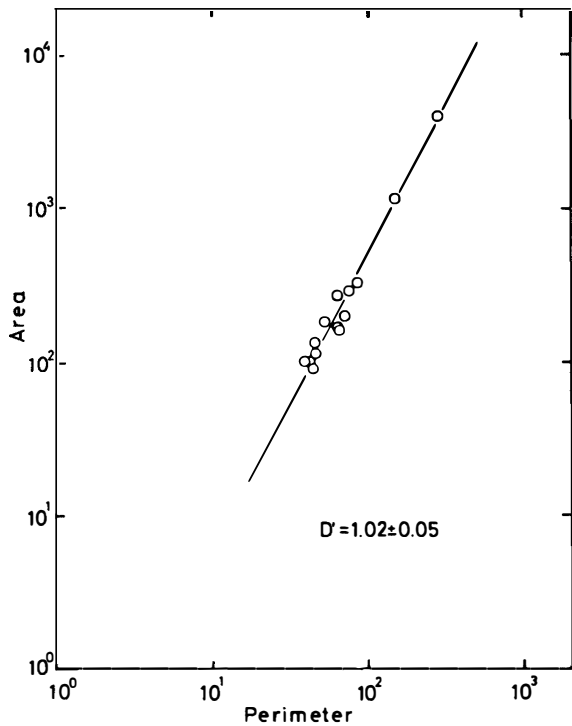


Fig. 9. Histogram of fractal dimensions D' of the parts surrounded by internal cracks.

Fig. 8. Area-perimeter relationship for the parts surrounded by internal cracks.

reflects the hierarchy nature of the fractal.

4.2. Glass sample

We have studied the fractal geometry of glass samples which are analyzed by the research group of Kobe University (NAKAMURA *et al.*, 1985).

We used two specimens from fragments produced by static uniaxial loading experiments. The obtained values of D' are very close to unity (1.020 and 1.021). The results on the impact-fractured surfaces are shown in Fig. 10, and show that the dynamic impact produces more irregular surfaces ($D'=1.08$) than the static loading. However, we cannot claim this with confidence, because the number of data on glass fragments is small. Moreover, it is found that the glass fragments possess two different appearances: "transparent" and "non-transparent". It is clear from the histogram inserted in Fig. 10 that the non-transparent glass fragments have larger fractal dimensions. The large fractal dimensions or the more irregular surfaces for non-transparent grains can be explained by higher density of the internal micro-cracks.

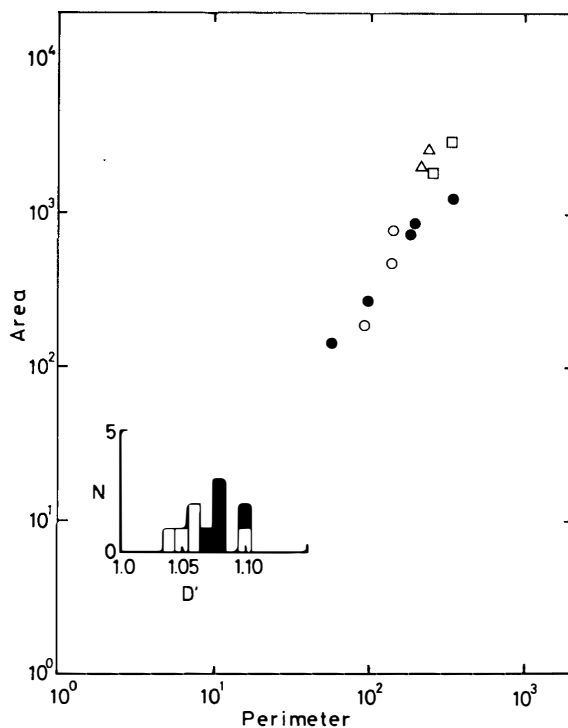


Fig. 10. Area-perimeter relationship for islands on the surfaces of impact-fractured glass. Open symbols represent transparent fragments and solid symbols represent non-transparent ones. Circles; Run No. 850510, triangles; Run No. 850528, squares; Run No. 850423-2. The histogram of fractal dimensions D' is also shown in the inset. Open bars and solid bars are for transparent and non-transparent fragments, respectively.

4.3. Application of the fractal dimension

In the present study, the fractal dimension is used as a basic quantity describing irregularity of fractured rock surfaces. The present result shows that two fracture-modes due to impact and static loadings have different fractal dimensions, and they can be distinguished from each other.

This result may enable us to classify, in terms of fractal dimension, the extraterrestrial rocks possessing the fracture surfaces arising from various degrees of impact and/or various degrees of tectonic deformation which took place in a parent body. The fractal geometry of the extraterrestrial rocks such as brecciated achondrites and some lunar rocks may provide significant constraint on the evolutionary history of each

parent body. The fractal dimension may be applicable to the classification of textural constituents of the extraterrestrial rocks, for example, lithic fragments, broken chondrules, fissures and/or veins in chondrites. In addition, the important information on the fractal geometry is carried by the outer shapes of the extraterrestrial materials of meteoroid to asteroid sizes which have not significant self-gravity effects, though the present experiments have used limited size.

In the actual processes on the surface of a planetesimal, however, the fracture of a rock involves both the catastrophic process of creating the fracture surfaces and the subsequent mechanical deformation and abrasion processes which potentially decrease the fractal dimension of the fracture surfaces. The temperature increase followed by the fracture process may also affect the shape of the fractured surfaces. Therefore, the fractal geometry of observed surfaces in natural rocks reflects the integrated effect of all factors associated with the fracture process. The appropriate combination of mineralogical, crystal-chemical and textural information (*e.g.*, FUJIMURA *et al.*, 1982, 1983) on the rock and the fractal geometry provides us with a useful and new line of approach for estimating the mechanical processes on the planetesimals.

Acknowledgments

We are grateful to Prof. N. FUJII of Kobe University for providing us with glass samples and their preprint. Our thanks are also due to Messrs. K. MASUDA and S. URAKAWA of Nagoya University for their support in operation of the deformation machine and the scanning electron microscope, respectively. We are indebted to Prof. M. KUMAZAWA of the University of Tokyo for critical reading of the manuscript.

References

- FUJII, N., MIYAMOTO, M., KOBAYASHI, Y. and ITO, K. (1982): On the shape of Fe-Ni grains among ordinary chondrites. *Mem. Natl Inst. Polar Res., Spec. Issue*, **25**, 319–330.
- FUJIMURA, A., KATO, M. and KUMAZAWA, M. (1982): Preferred orientation of phyllosilicates in Yamato-74642 and -74662, in relation to deformation of C2 chondrites. *Mem. Natl Inst. Polar Res., Spec. Issue*, **25**, 207–215.
- FUJIMURA, A., KATO, M. and KUMAZAWA, M. (1983): Preferred orientation of phyllosilicate [001] in matrix of Murchison meteorite and possible mechanisms of generating the oriented texture in chondrites. *Earth Planet. Sci. Lett.*, **66**, 25–32.
- FURUMOTO, M., FUJIMURA, A., TAKAGI, Y. and MIZUTANI, H. (1984): Fractal dimensions of rock fragments. *Proc. ISAS Lunar Planet. Sci. Symp.*, 17th, 25–26.
- MANDELBROT, B. B. (1982): *The Fractal Geometry of Nature*. San Francisco, Freeman, 460 p.
- MANDELBROT, B. B., PASSOJA, D. and PAULLAY, A. (1984): Fractal character of fracture surfaces of metals. *Nature*, **308**, 721–722.
- MASUDA, K. (1984): Experimental studies of strain-rate dependence and pressure dependence of failure properties of granite. Master Thesis of Nagoya University.
- MIZUTANI, H., KUMAZAWA, M., KATO, M., MASUDA, T., KAWAKAMI, S., TAKAGI, Y. and KANI, K. (1981): Performance tests of the high velocity shock gun with a novel sabot stopper. *Proc. ISAS Lunar Planet. Sci. Symp.*, 14th, 267–277.
- NAKAMURA, H., NII, Y., ITO, K., FUJII, N. and MATSUDA, J. (1985): Fractal dimension of fracture surfaces as a measure of the intensity of fracturing. *Nature* (in press).
- TAKAGI, Y., MIZUTANI, H. and KAWAKAMI, S. (1984): Impact fragmentation experiments of basalts and pyrophyllites. *Icarus*, **59**, 462–477.

(Received July 5, 1985; Revised manuscript received October 28, 1985)